Original

Abibe, A.B.; Amancio-Filho, S.T.; dos Santos, J.F.; Hage, E.jr.;

Development and Analysis of a New Joining Method for Polymer–Metal Hybrid Structures

Development and Analysis of a New Joining Method for Polymer-Metal Hybrid Structures

A.B. Abibe, S.T. Amancio-Filho, J.F. Dos Santos and E. Hage, jr

Development and Analysis of a New Joining Method for Polymer–Metal Hybrid Structures

A. B. Abibe

Postgraduation Program in Materials Science and Engineering (PPG-CEM), Department of Materials Engineering (DEMa), Federal University of Sao Carlos (UFSCar), Rodovia Washington Luiz km 235, Sao Carlos-SP, Brazil

S. T. Amancio-Filho*

GKSS Forschungszentrum Geesthacht GmbH, Institute of Materials Research, Materials Mechanics, Advanced Polymer-Metal Hybrid Structures, Max-Planck-Strasse 1, D-21502 Geesthacht, Germany

J. F. Dos Santos

GKSS Forschungszentrum Geesthacht GmbH, Institute of Materials Research, Materials Mechanics, Solid State Joining Processes (WMP), Max-Planck-Strasse 1, D-21502 Geesthacht, Germany

E. Hage Jr

Department of Materials Engineering (DEMa), Federal University of Sao Carlos (UFSCar), Rodovia Washington Luiz km 235, Sao Carlos-SP, Brazil

ABSTRACT: The influence of innovative technologies and green policies in manufacturing has created new design needs. Reinforced thermoplastics and metals are widely used as engineering materials for weight reduction, usually assembled by joining. This article presents the principles of a new injection clinching joining (ICJ) process for polymer–metal hybrid structures. Based on staking, injection molding, and adhesive bonding technologies, ICJ provides spot joints with mechanical anchoring of a polymeric partner in a designed cavity of a metallic part. A feasibility study on a

---

polyamide thermoplastic composite and aluminum is presented, addressing the mechanical, microstructural, and thermal properties of ICJ joints.

INTRODUCTION

SINCE THE SECOND World War, plastics have become increasingly popular due to their combination of low weight and good mechanical properties. Specific needs in various industrial fields have led to deeper research into the combination of dissimilar materials. Thermoplastic composites have found even wider areas of application, because they offer high strengths, yet they are light in weight and low in cost [1–3]. New designs and combinations of parts eventually require components to be joined somehow, and new techniques have emerged in recent years. Unlike the preceding technologies of thermoset matrix composites, thermoplastic composites are increasingly favored for high-end applications. With their faster processing, high-delaminating resistance, excellent chemical resistance, and greener environmental behavior, they have become the preferred alternative for demanding technical applications [4]. Due to this evolution of material choices, it is a constant challenge to assemble the structures with the required quality and performance.

The prevailing joining methods are adhesive bonding and mechanical fastening [5–7]. These processes suffer limitations, such as stress concentration, extensive surface preparation, extra weight, and environmental emissions [8,9]. Promising techniques have arisen to solve these issues. Staking techniques, for example, are successfully used to join dissimilar materials. Staking consists of a stud projecting from a surface of one of the joining partners (thermoplastic) and a geometrically compatible hole on the surface of the joint partner (any material) [10]. After the assembly of the stud into the hole, energy is applied to the stud to soften it. The stud is deformed by a tool, producing a rivet-like element and mechanically anchoring both parts. Types of staking include cold staking, heated-tool staking, hot-air staking, ultrasonic staking, and infrared/ laser staking, according to the type of energy provided to soften the stud [10–12]. Even though these methods are in use industrially [13], their field of application is sometimes limited. Moreover, cold and hot techniques staking present problems with elastic recovery of the polymer, while ultrasonic and IR/ laser staking techniques require costly equipment and IR/laser staking works only with optically compatible plastics. Since these methods are still finding their niches and the search for lighter structures continues, there remains scope for the introduction of alternative joining technologies for polymer–metal hybrid structures.

This article intends to present injection clinching joining (ICJ) [14], a new joining method for staking polymer–metal hybrid parts, describing the principles of this process in terms of controlling parameters, structure–property relations, and potential applications. A feasibility study of commercially available fiberglass-reinforced polyamide 66 (PA66/FG30%) and aluminum AA 2024-T351 is also included. In summary, a critical analysis of the advantages, limitations and viability of the technique is presented.

MATERIALS

The parts used for this study were 10-mm thick extruded PA66/FG30% plaques and 4-mm thick extruded AA 2024-T351 plates, both of which were machined to the shapes shown in Figure 1(a). The polymeric part has a 7 mm high, 9 mm diameter stud protruding from its surface, which fits into the machined profiled hole on the metallic part (Figure 1(b)). Overlap samples of similar geometries were produced to test the mechanical performance of the joints through lap shear testing (Figure 1(c)).

\Neat polyamide 66 (PA66), also known commercially as 'nylon 66', is a semi-crystalline engineering thermoplastic known for its good mechanical, dimensional stability, and tribological properties. Additional reinforcement by glass fibers greatly increases the stiffness, strength, dimensional stability, and resistance to creep at high temperatures [15]. A large assortment of grades, with combinations of additives for glassfiber-reinforced PA66 is available,
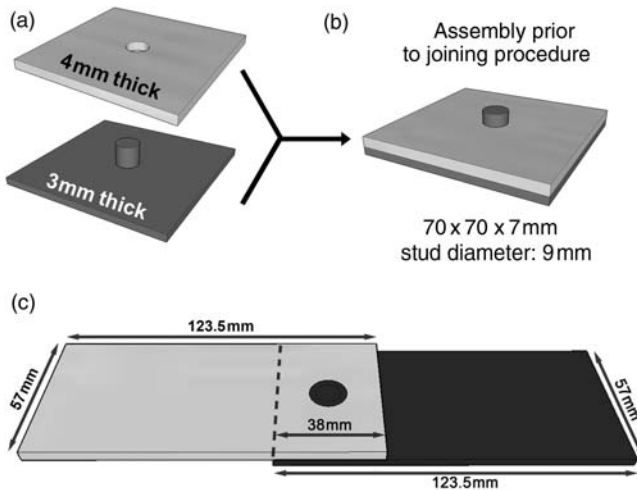

Figure 1. *Configuration of ICJ spot-like joints: (a) individual joining partners; (b) joining partners positioned; and (c) overlap specimen for bearing stress measurement.*

depending on its intended application. The PA66/FG30% grade used in this study is a heat-stabilized polyamide 66, reinforced with 30% glass fibers by weight. Tensile strength ranges from 50 to 100 MPa, depending on the moisture content of the nylon [15]. For tribology, the coefficient of friction is greatly reduced, compared to the non-reinforced material, but usually at the expense of increased wear rate after excessive wear has been experienced [16,17], and this is one of the most attractive features of the material. It has a high melting temperature (260°C) and retains good mechanical properties under high-temperature conditions, having a maximum service temperature in air at 120°C for long periods (5000–20,000 h), or up to 240°C for time spans of several hours [18]. Generally, PA66/FG30% has a high deflection temperature under load, low coefficient of thermal expansion, enhanced fatigue and vibration resistance over a wide temperature range, efficient dielectric properties, and good chemical resistance [15]. Polyamides are highly hygroscopic; hence all these properties may exhibit significant variation, depending on the moisture content of the material [19]. It is applied in a wide range of industries, particularly the automotive and electrical, with the former being the most notable. Its excellent high-temperature properties, wear and chemical resistance, processing ability and strength meet the needs of the demanding automotive market and its utilization is increasing with a trend of replacing heavier metallic parts with lighter and equally capable plastic components.

Aluminum 2024 is a wrought heat-treatable alloy of the 2000 aluminum series. The main alloy elements for this series are Cu and Mg. Specifically, the AA2024-T351 is a solution heat-treated at 495°C, cold-worked, naturally aged alloy with a final stretching step for stress release. It has good tensile strength and fair stress corrosion resistance [20]. Copper is added to increase strength, to support precipitation hardening, and to improve ductility and welding ability. Magnesium increases the strength by means of solid-solution strengthening and improves work-hardening ability [21]. This alloy is also characterized by poor corrosion resistance, very low extrusion ability and poor welding ability by fusion techniques [22]. It is one of the most important aeronautical alloys, nowadays; being used by aircraft producers such as Embraer, Eclipse, and Bombardier [21]. Additionally, it is used on gears and shafts, hydraulic valve bodies, missile parts, pistons, and fastening devices.

METHODS

A prototype-joining unit, specially designed for the ICJ process and placed on a standard hydraulic press, was used for this study. The prototype consists of a heating unit, which controls the temperature of resistance-heated ceramic rings placed around a hot case. A system including a
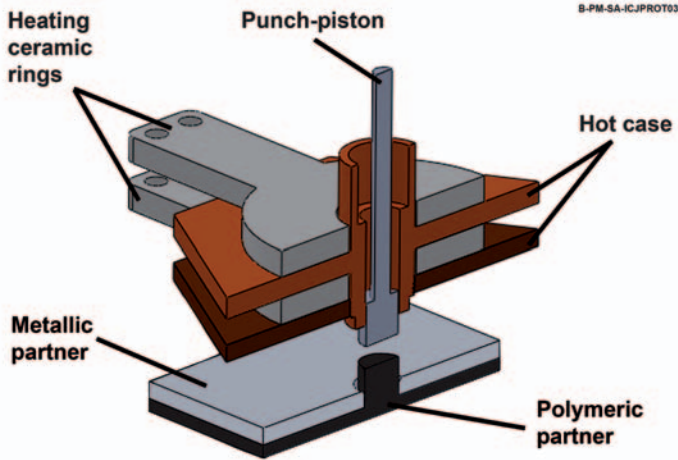
Figure 2. *Illustration of ICJ prototype.*
Note: The punch-piston is assembled co-axially to the hot case and heating elements.
The metallic partner is placed on top of the polymeric partner.

punch-piston assembled co-axially with the hot case is used to clamp the joining partners prior to processing (Figure 2).

In order to record the temperature history during processing, the joints are thermally monitored by an infrared thermo-camera (Jenoptiks Variotherm, Germany) pointing directly on the hot case involving the polymeric stud. A force measuring system was coupled to the joining system to allow the measurement of the joining force. The overall concept for the joining system is shown as a block chart in Figure 3. The joined samples were cut and subjected to standard materialographic procedures of grinding and polishing, in order to observe the microstructural features on a light microscope. These samples had their local mechanical properties determined by microhardness testing. Lap shear tests were performed on overlap joints for the evaluation of the bearing strength, according to the standard ASTM D 5961 [23], and evaluated according to the controlling parameters used in the joint production. Bearing stresses were calculated using Equation (1) [23]:

$$\sigma_i = \frac{P_i}{k \times D \times h}, \tag{1}$$

where σ_i is the bearing stress in megapascals at a given data point, P_i the load in Newton at a given data point, k a force per hole factor (1.0 for single
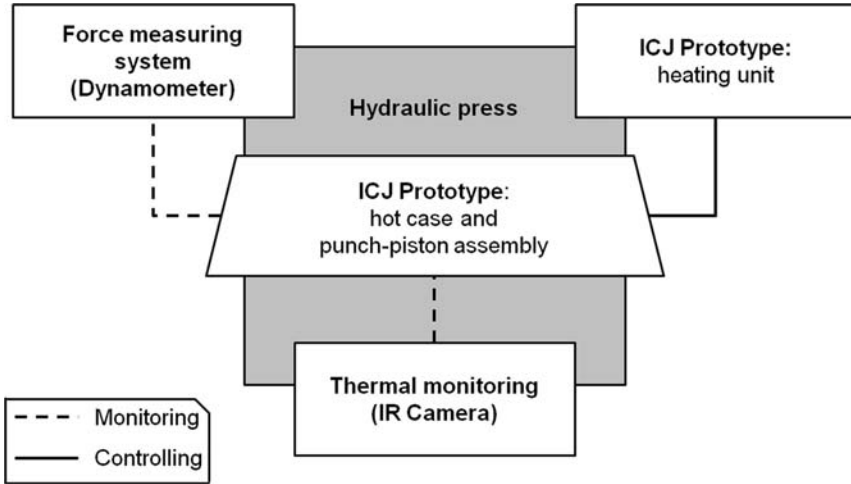
Figure 3. *Block chart describing the ICJ equipment assembly for joining.*
Note: The joining assembly is placed in a hydraulic press and is monitored during joining by a dynamometer and an IR camera. Temperature is controlled by a heating unit.

joining point systems), D the diameter of the hole in millimeters, and h the thickness of the joined plate in millimeters. Strain of the tested joints was measured through the change in length per unit of the original length using an extensometer.

PRINCIPLES OF THE ICJ METHOD

ICJ is a new spot joining process for hybrid structures composed of thermoplastics and metals or thermoset polymers [14]. The technique is based on the principles of injection molding, staking, and adhesive bonding. Joints are produced by the heating and deformation of a thermoplastic element (normally a cylindrical stud) inserted into a through hole (cavity) placed in the metallic/thermoset component. This creates a rivet by using part of the structure itself, resulting in weight savings and improved mechanical reliability.

The ICJ spot-like joint configuration relies on optimized mechanical anchoring of the formed rivet. The polymeric stud can be either machined or injection molded to the desired final shape, which is more suitable for mass production. The designed hole can be plain or profiled (e.g., threaded) or have a combination of these features. For a better mechanical interlocking of the polymer, the hole is usually tapered in order to increase the anchoring area of the rivet.
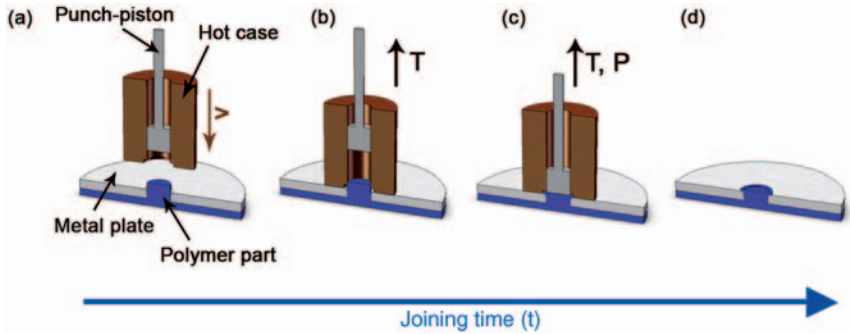
Figure 4. *Stages of the ICJ process: (a) tool approaching, (b) hot case heats the polymer, (c) forging pressure applied by the piston, (d) joined part.*

A detailed illustration of the process is shown in Figure 4. The joining partners are first assembled together, with the polymeric stud inserted into the hole of the metallic/thermoset partner. The tool approaches the parts (Figure 4(a)); the hot case encloses the polymeric stud, and heats it up to the designed processing temperature (Figure 4(b)). At the end of the heating phase, the punch-piston applies a forging pressure on the softened/molten polymeric stud, forcing it into the cavities in the metallic partner's hole (Figure 4(c)). Pressure is maintained to decrease polymer relaxation as the system is air-cooled. After cooling, the tool retracts and the joint is consolidated (Figure 4(d)).

Controlling Parameters and Variables

The main controlling parameters of the ICJ process are the heating time, the processing temperature, and the injection rate. Also important are cavity geometry and material properties, such as structural water in polyamides, molten viscosity, and transition temperatures. *Heating time* is the period during which the hot case heats the polymeric stud to the desired *processing temperature*. Both these parameters will influence the amount of heat transferred to the polymeric stud, hence its softened molten viscosity, making it easier or harder to deform. The *injection rate* is the rate at which the punch-piston moves toward the softened polymeric stud, injecting it into the designed hole. Since higher deformation rates lower the viscosity of a pseudo-plastic fluid through shear thinning (increasing softened/molten polymer flowability) [24], this will influence the required joining force in order to form the rivet.

The main variables observed during the process are joining force and cavity filling. *Joining force* is the measured load transferred by the

punch-piston to the softened polymeric stud in order to inject it into the cavities of the hole in the metallic/thermoset component. The force is dependent on the amount of heat transferred to the stud and the deformation rate. These factors will directly affect the viscosity of the polymer. Heat provides movement of the polymeric chains, reinstating the transition from glassy state to a viscous liquid, while increasing deformation rate will lower viscosity, increasing the flowability of the polymer [24]. *Cavity filling* is associated with the filled cavity volume compared to the total cavity volume. The design of the hole ensures that full cavities provide more efficient anchoring, an influential factor for optimal joint performance. This variable will also be influenced by the rheology of the softened/molten material, because the less viscous it is the better the polymer flow to the inside of the cavities.

Joint Microstructure

During processing, heat and deformation modify the microstructure of the materials and therefore their properties. Figure 5 shows the microstructural zones of a typical ICJ joint. Deformation drastically modifies at least a portion of the polymeric stud, creating a polymer thermo-mechanically affected zone (PTMAZ). The greatest concentration of macrostructural and microstructural changes, such as cavity filling and hydrostatic formation of flow lines and voids, is found in this volume area. The volume around the PTMAZ may be influenced by heat transfer and is identified as a polymer-heat affected zone (PHAZ). Although the
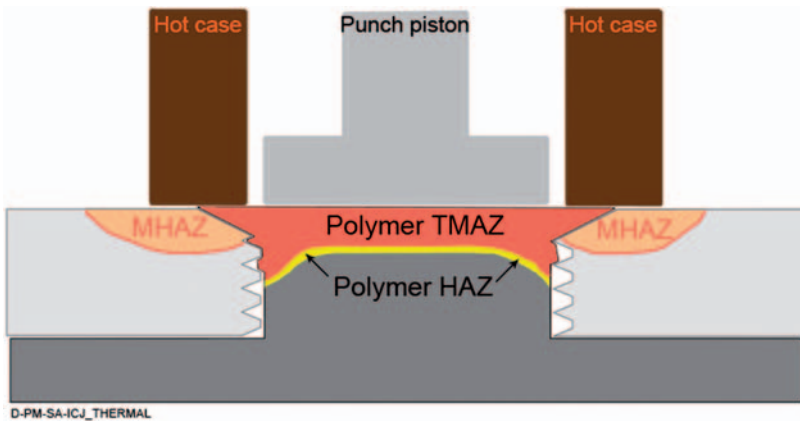

Figure 5. *Thermal zones of an ICJ joint.*
Note: Since the extent of the effect of the process on the PHAZ is not known, it is indicated as a thin line.

phenomena taking place in the PHAZ are still not fully understood, it seems that there are no visual changes in comparison with the base material. The heat may also generate a heat-affected zone in the metallic component (MHAZ). Depending on the metallic alloy used and its composition, high temperatures may lead to annealing phenomena and other metallurgical processes changing material strength in this zone.

RESULTS AND DISCUSSIONS

Feasibility Study on Polyamide 66/FG30% and Aluminum 2024-T351

A preliminary ICJ joining ability study was designed, based on the crystalline melting point (260°C) [18] and degradation range (>320°C) [25] of the glass-reinforced polyamide 66/FG30%, as well as on the annealing temperature (415°C) [20] of the alloy AA2024-T351. Intended to determine the optimal ICJ-controlling parameter ranges for this material combination, an investigation was carried out with various heating times and processing temperatures [26]. Joints were obtained within the following processing parameter ranges: processing temperatures of 250–300°C, and heating times of 0.25–3 min. The forging pressure was controlled with the piston of a hydraulic press and the joining force was monitored by the load measuring system.
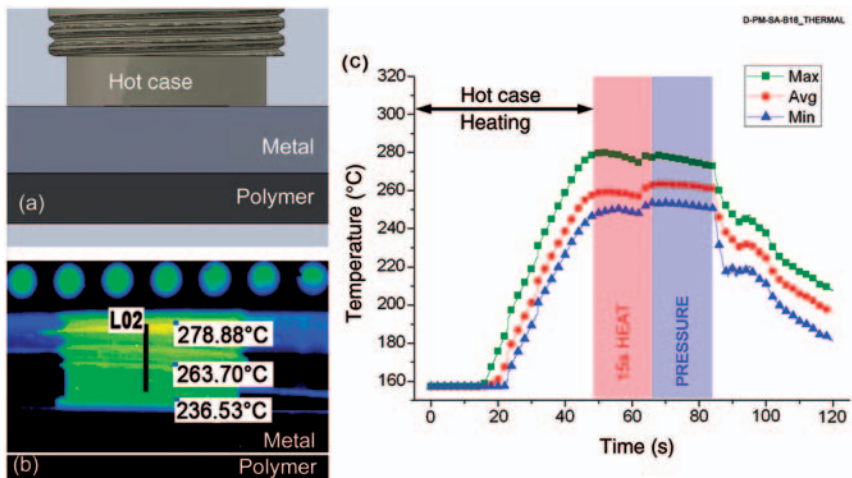

Figure 6. *Thermal monitoring of a sample processed at 275°C with a 0.25 min (15 s) heating time: (a) illustration showing the elements involved in thermal measurements; (b) peak temperatures of the hot case and measurement line for the curve in (c); and (c) full-cycle plot with maximum, minimum, and average temperatures through the line 'L02' in (b).*
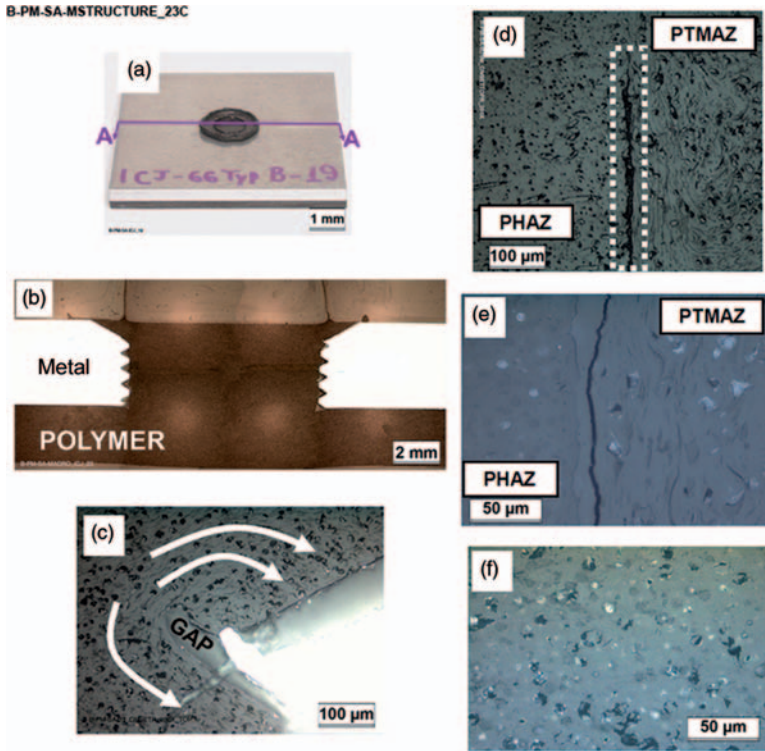
Figure 7. *Microstructure highlights of ICJ: (a) surface view; (b) joint cross-section (16×); (c) polymer–metal interface, with arrows indicating molten-polymer flow around the thread flight (200×); (d) polymer–polymer interface between PHAZ and PTMAZ (200×); (e) PHAZ and PTMAZ interface (500×); and (f) PA66/FG30% base material (500×).*

The temperature history was recorded shortly before the injection stage, detecting the temperatures on the hot case and the joining partners. Figure 6 shows this measurement area, with examples of a thermograph and the temperature history during the full joining cycle of a specimen joined at 275°C in 0.25 min (15 s).

A typical macrograph of a specimen was produced at 250°C in 3 min (180 s) with threaded-cavity geometry and it is tapered in the upper portion, as shown in Figure 7. The specimen was cut across the mid-section of the joint and studied under light optical microscopy, as shown in Figure 7(a). It is known that thermal processing can induce void formation and other thermal flaws in polyamides due to moisture evolution [27]. Specimens produced at 300°C had good cavity filling, but showed voids on the deformed stud and a large loss of polymer mass to the surroundings of the

rivet head. Joints produced at lower temperatures usually had sound rivet heads in the tapered cavity area (Figure 7(b)) [26]. The interface between the injected polymer front and the metal frequently shows interesting features, as shown in Figure 7(c). In this figure, arrows indicate the molten polymer flow into the cavity around a thread flight. Furthermore, a gap located in the consolidated molten front near the tip of the thread flight was noted, probably explained by differential shrinkage during cooling due to the large difference in thermal expansion of the polymer and metal. In Figure 7(d), a dashed rectangle highlights a polymer–polymer interface between the polymeric stud and the molten polymer front. This interface is characterized by a weld line formed during cooling. It also delineates the transition between the PTMAZ (the molten polymer front) and PHAZ. In the PTMAZ, it is possible to observe induced flow lines, thermal voids, and small consolidation cracks (Figure 7(e)). In the PHAZ, the appearance of the polymer was very similar to the base material (Figure 7(f)). The same lack of distinction was shown to take place in the regions around the cavity in the aluminum partner.

Microhardness testing was performed on the materialographic specimens according to ASTM E384-992e1 [28] and the procedure described in the literature [29], to evaluate the local mechanical properties of the ICJ joints. An indentation load of 0.495 N and a holding time of 15 s were applied during testing. In each specimen, testing was performed by defining five lines of indentations, as shown in Figure 8(a). Comparing the experimental base material average hardness (14.3 HV for PA66/FG30% and 135.7 HV for AA2024-T351), a slight decrease in the average hardness of the metal can be seen, while in the polymer, a small increase in average hardness is observed on the top of the polymeric stud (see curve '6 mm' at the distance to center of −3 and 3 mm, Figure 8(a)), where the polymer experienced the strongest thermo-mechanical treatment.

This feature may be more easily seen from a microhardness distribution contour plot. Figure 8(b) shows a cross-section macrograph of the sample in Figure 7, with the left hand side showing the etched aluminum alloy and the microhardness distribution map of the processed polymer, while on the right hand side there are non-etched polymer and the microhardness distribution map of the metallic plate. These results (as indicated by the rectangle in Figure 8(b)) show that the processing only slightly affects the local mechanical properties of the molten-flowed polymer and no direct changes in hardness of the polymeric stud could be observed. It was also impossible to identify the PHAZ and MHAZ extensions by this technique. The selection of other analytical techniques such as nano-indentation and wide angle X-ray diffraction (WAXS) may provide further information on the dimensions of these microstructural zones and if any preferential orientation
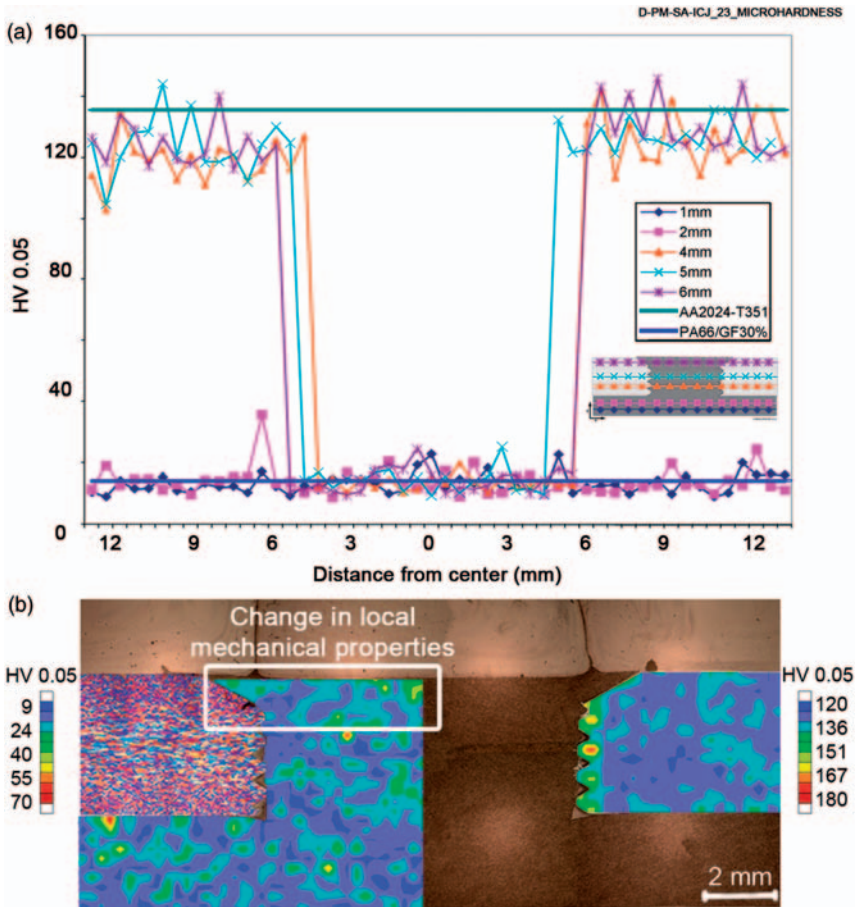
Figure 8. *Microhardness distribution of the ICJ joint of Figure 7: (a) indentation line profiles of the specimen and average hardness of base materials (straight lines); and (b) contour plot of the same sample, showing a superposition of micrographs and the respective microhardness distribution maps.*

of the polymer chains was induced, which can directly relate to the local strength. The slightly higher average hardness in the threaded metallic cavity region is associated with mechanical hardening induced by the thread cutting operation.

Overlap samples (Figure 1(c)), with a geometry based on standard DIN 50124 [30], were tested at room temperature and 2 mm/min traverse speed in a ZWICK 1478 universal testing machine (100 kN loading cell), for the evaluation of bearing strength. The clamps of the machine were aligned to the longitudinal axis of the plates without using additional fixtures.
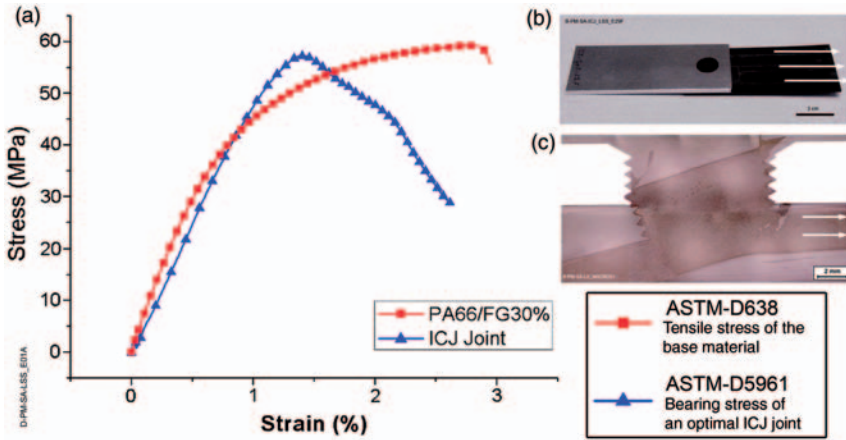
Figure 9. *(a) Average engineering stress–strain tensile curve of five tested specimens [31] for PA66/FG30% and a bearing stress–strain curve [23] for an optimal ICJ joint; (b) overlap specimen before testing; and (c) the cross-section of tested sample; arrows indicate the pulling direction.*

Three specimens were tested for each condition. For evaluation of the stresses endured by the samples, standard ASTM-D5961 [23] for riveted structures was selected. At optimal parameter conditions (300°C and 3 min), the maximum bearing load measured was greater than 2 kN; the average bearing load for this joint was 1.8 ± 0.3 kN. Bearing stresses (from Equation (1) [23]) endured by the joints reached about 97% of the polymeric base material ultimate tensile strength calculated from ASTM-D638 [31] (Figure 9). The joint with worst performance endured 835 N of bearing load, meaning 35% of the polymeric base material's ultimate tensile strength.

Lap shear specimens of overlap joints produced with as-received polyamide failed by 'rivet pull-out' of the polymeric stud from the plate (Figure 10(a)). Further investigation has shown that joints having heat-treated polyamide components prior to joining will fail (Figure 10(b)) by 'net-tension' [32] in the polymer area instead of 'rivet pull-out,' due to a decrease in the overall ductility associated with structural water elimination.

FINAL REMARKS

The principles of the ICJ method were presented in this study through a feasibility study of joints produced with AA 2024-T351 and PA66/FG30%. Typical ICJ joint microstructural features, local mechanical properties (microhardness), bearing strength, and structure–property relationships were evaluated.
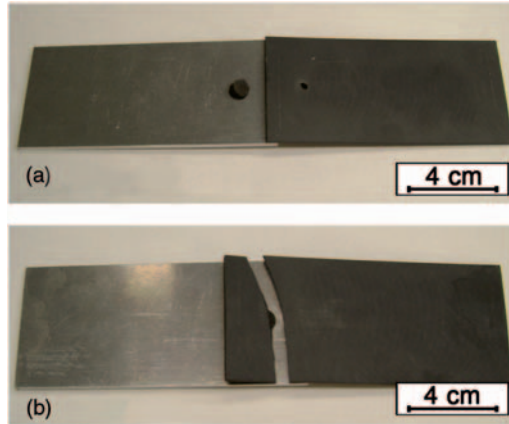
Figure 10. *Fracture modes of ICJ joints (bottom view): (a) complete rivet pull-out failure; and (b) net-tension failure.*

   Mechanical anchoring was revealed to be an influential parameter on joint strength. This means cavity filling is necessary for higher joint strength, which implies that appropriate selection improved cavity geometries. The design of improved cavities should also consider the rheology properties and thermal behavior of the processed polymer. Sound joints appear to be produced at higher temperatures and longer times, by which heating performance is increased, hence decreasing molten viscosity of the stud and enhancing material flow into the cavity.
   Microhardness investigation was not able to provide detailed information on the extent of any local strength changes related to thermo-mechanical processing. The selection of advanced analytical techniques such as nano-indentation and wide angle X-ray diffraction (WAXS) may provide a better understanding of local mechanical strength in ICJ joints. A high average lap shear strength of up to 97% of the polymeric base material's ultimate tensile strength was achieved. Further investigation indicated that the presence of structural water, in the case of hygroscopic polymers such as the PA66/FG30%, affects the ICJ joint performance as well as its failure mechanisms (by rivet pull-out for as-received joints and by net-tension for the heat-treated polyamide joints, as shown in Figure 10). This behavior is probably related to a reduction of ductility due to water elimination. Additional investigation on the failure mechanisms is in progress.
   Since this process competes with current joining technologies, mainly adhesive bonding, staking, and mechanical fastening, it is useful to address some of its advantages and limitations. Its advantages are: (a) it needs little surface preparation; (b) simple technology is required; (c) it is an

environment-friendly technique, producing no gases or fumes; d) it saves costs by using only the joining partners without requiring extra parts; e) it provides good mechanical anchoring in designed holes; (f) it requires one-side accessibility; (g) it is applicable to industrial lines [14]; and (h) it has excellent mechanical performance.

However, compared to the other methods, some limitations are noticed, mainly (a) only spot joints are possible; (b) it is a permanent joining method; (c) it is not feasible with thermosets; (d) differential thermal expansion of joining partners makes larger assemblies tricky; and (e) it needs longer cycle times with thermally resistant thermoplastics. Furthermore, the current ICJ prototype operates with an electric heating unit. A prototype frictional heating unit is currently being developed. This will allow future energy and cost savings associated with a decrease in assembly and joining times.

New environmental policies and increased safety requirements make the transport industry a good niche for polymer–metal hybrid structures. As examples, ICJ could be successfully applied in aluminum/reinforced thermoplastic hoods and front-ends [33,34] that also involve thermoplastic composite/metal joints.

This study shows that ICJ is a promising alternative joining technology for polymer–metal hybrid structures. The excellent mechanical properties, good aesthetics, environment-friendly processing and promise of energy and material efficiencies make this process a good alternative to current joining technologies.

ACKNOWLEDGMENTS

REFERENCES

1. Brydson, J.A. (1999). Additives for Plastics, In: Brydson, J.A. (ed.), *Plastics Materials*, **7th edn**, pp. 124–155, Butterworth-Heinemann, Oxford, England.

2. Chawla, K.K. (1998). Introduction, In: Chawla, K.K. (ed.), *Composite Materials: Science and Engineering*, **2nd edn**, pp. 3–5, Springer-Verlag, New York, NY, USA.

3. Friedrich, H.E. (2003). Challenges of Materials Technology for Low-Consumption Vehicle Concepts, *Advanced Engineering Materials*, **5**(3): 105–112.

4. Berglund, L.A. (1998). Thermoplastic Resins, In: Peters, S.T. (ed.), *Handbook of Composites*, **2nd edn**, pp. 115–128, Chapman & Hall, London, England.

5. Kim, S.S., Yu, H.N. and Lee, D.G. (2007). Adhesive Joining of Composite Journal Bearings to Back-Up Metals, *Composites Science and Technology*, **67**: 3417–3424.

6. Thoppul, S.D., Finegan J. and Gibson, R.F. (2008). Mechanics of Mechanically Fastened Joints in Polymer–Matrix Composite Structures – A Review, *Composite Science and Technology*, **69**: 301–329.

7. Adams, R.D., Comyn, J. and Wake, W.C. (1997). Introduction, In: Adams, R.D., Comyn, J. and Wake, W.C. (eds), *Structural Adhesive Joints in Engineering*, **2nd edn**, pp. 7–11, Chapman & Hall, London, England.

8. Ageorges, C., Ye, L. and Hou, M. (2001). Advances in Fusion Bonding Techniques for Joining Thermoplastic Matrix Composites: A Review, *Composites Part A*, **32**: 839–857.

9. Baldan, A. (2004). Review Adhesively-Bonded Joints and Repairs in Metallic Alloys, Polymers and Composite Materials: Mechanical and Environmental Durability Performance, *Journal of Materials Science*, **39**: 4729–4797.

10. Rotheiser, J. (2004). Staking/Swaging/Peening/Cold Heading/Cold Forming, In: Rotheiser, J. (ed.), *Joining of Plastics: Handbook for Designers and Engineers*, **2nd edn**, pp. 428–434, Carl Hanser Verlag, Munich, Germany.

11. Yeh, H.J., Schott, L.C. and Park, J.B. (1998). Experimental Study on Hot-Air Cold Staking of PC, PC/ABS and Acetal Samples, In: *SPE ANTEC' 98*, Atlanta, USA, April 27 to May 1.

12. Hahn, O. and Finkeldey, C. (2003). Ultrasonic Riveting and Hot-Air-Sticking of Fibre-Reinforced Thermoplastics, *Journal of Thermoplastic Composite Materials*, **16**: 521–528.

13. Kirkland, T.R. (2002). Joining Applications in Exterior Automotive Panels Made of Thermoplastic Olefin, In: *SPE ANTEC' 02*, San Francisco, USA.

14. Amancio-Filho, S.T., dos Santos, J.F. and Beyer, M. (2010). Method and Device for Connecting a Plastic Workpiece to a Further Workpiece, US Patent 7,780,432 B2.

15. Kohan, M.I. (ed.) (1973). Modified Nylons, In: *Nylon Plastics*, **1st edn**, pp. 430–436, John Wiley & Sons, New York, USA.

16. Hooke, C.J., Kukureka, S.N., Liao, P., Rao, M. and Chen, Y.K. (1996). Wear and Friction of Nylon-glass Fibre Composites in Non-Conformal Contact Under Combined Rolling and Sliding, *Wear*, **197**: 115–122.

17. Kukureka, S.N., Hooke, C.J., Rao, M. Liao, P. and Chen, Y.K. (1999). The Effect of Fibre Reinforcement on the Friction and Wear of Polyamide 66 Under Dry Rolling-Sliding Contact, *Tribology International*, **32**: 107–116.

18. Product Data Sheet (2007). ERTALON® 66-GF30 (Quadrant AG), p. 1. Available at http://epp.quadrantplastics.com/default.aspx?pageid=914 (acessed date October 5, 2010).

19. Jia, N. and Kagan, V.A. (2000). Mechanical Performance of Polyamides with Influence of Moisture and Temperature-Accurate Evaluation and Better Understanding, In: *SPE ANTEC' 00*, Orlando, USA.

20. Davis, J.R. (ed.) (1996). Wrought Products, In: *Aluminium and Aluminium Alloys*, **3rd edn**, pp. 60, 76, 81, ASM International, Materials Park, OH, USA.

21. Mathers, G. (2002). Material Standards, Designations and Alloys, In: Mathers, G. (ed.) *The Welding of Aluminium and its Alloys*, **1st edn**, pp. 35–37, Woodhead Publishing Limited, Cambridge, England.

22. Weis Olea, C.A. (2008). Influence of Energy Input in Friction Stir Welding on Structure Evolution and Mechanical Behaviour of Precipitation-hardening in Aluminium Alloys (AA2024-T351, AA6013-T6 and Al-Mg-Sc), PhD Thesis, Ruhr-Universität Bochum, GKSS-Forschungszentrum.

23. D 5961/D 5961M-08 (2008). Standard Test Method for Bearing Response of Polymer Matrix Composite Laminates, ASTM International, West Conshohocken, PA.

24. Dealy, J.M. and Wissbrun, K.F. (1999). Steady Simple Shear Flow and the Viscometric Functions, In: Dealy, J.M. and Wissbrun, K.F. (eds), *Melt Rheology and its Role in Plastics Processing: Theory and Applications*, **1st edn**, pp. 3–37 and 153–176, Kluwer Academic Publishers, Dordrecht, The Netherlands.

25. Material Safety Data Sheet (2003). ERTALON® 66-GF30 (Quadrant AG). pp. 1–3, available online at http://epp.quadrantplastics.com/default.aspx?pageid=914 (acessed on 05/10/2010).
26. Abibe, A. (2009). GKSS Internal Report WM/WMP/002.09. Public access available upon request. Please contact S. Amancio-Filho.
27. Jia, N. (2002). Effects of Moisture Conditioning Methods on Mechanical Properties of Injection Molded Nylon 6, In: *SPE ANTEC' 02*, San Francisco.
28. ASTM E384-992e1 (2005). Standard Test Method for Microindentation Hardness of Material, ASTM International, West Conshohocken, PA.
29. Calleja, F.J.B. and Fakirov, S. (2000). Microhardness Determination in Polymeric Materials, In: Calleja, F.J.B. and Fakirov, S. (eds), *Microhardness of Polymers*, **1st edn**, pp. 11–33, Cambridge University Press, Cambridge, England.
30. DIN 50124 (1977). *Scherzugversuch an Widerstandspunkt – Widerstands -buckel - und Schmelzpunktschweiss-verbindungen*, Deutsche Institut für Normung eV, Germany.
31. D 638-01 (2001). Standard Test Method for Tensile Properties of Plastics, ASTM International, West Conshohocken, PA.
32. York, J.L., Wilson, D.W. and Pipes, R.B. (1982). Analysis of the Net Tension Failure Mode in Composite Bolted Joints, *Journal Reinforced Plastics and Composites*, **1**: 141–152.
33. Anon. (2004). Ford Focus Van Features Hybrid Metal/Composite Front-end, *Reinforced Plastics*, **48**(8): 4.
34. Goldbach, H. and Hoffner, J. (1997). Hybridbauteil in der Serienfertigung: Designsbeispiel Frontend, *Kunststoffe*, **87**(9): 1133–1138.